rr - 142
SSCL-PP-142

ANALYSIS OF MONOFILAMENT AND MULTIFILAMENT SAMPLES OBTAINED FROM PHASE I OF THE SSCL VENDOR QUALIFICATION PROGRAM

J. M. Seuntjens, V. A. Bardos, D. C. Christopherson, D. W. Capone II, F. Y. Clark, E.S. Coleman, M. J. Erdmann, T. J. Headley*, B. Jones, V. Levy, and D. K. Washburn
SSC Laboratory, MS 1005
Dallas, TX 75237

DRAFT

*Sandia National Laboratories
Division 1822
Albuquerque, NM 87185-5800

INTRODUCTION

Select samples from each cable vendor in the SSC Laboratory Vendor Qualification Program were characterized by a series of mechanical and metallographic tests. Samples were chosen to cover the spectrum of monofilament types in each vendor's process. The tests performed are NbTi alloy hardness, tensile strength of the restack element, tensile properties of the restack element without the copper, copper to superconductor ratio, barrier X-ray line scans, and NbTi alloy and Nb barrier image analysis. Process data supplied by each cable vendor is also analyzed and extrusion k factor and monofilament and multifilament yield data are analyzed. This report summarizes the data available to date without revealing company sensitive information.

EXPERIMENTAL PROCEDURE

Metallographic and Mechanical Tests

Hardness- Metallurgical mounts were made of transverse sections of select samples and polished through 0.5 micron. 5 Vickers microhardness readings were made on each monofilament using a Leco M-400-G1 Hardness tester and a 100 g load with a 15 second duration. For each sample, the coefficient of variation (Cv) was less than 2% for the 5 measurements.

Tensile tests- Standard tensile tests were performed on the restack elements, both as-received and after removing the copper in a solution of 50/50 nitric acid / de-ionized water, as well as as-received finished strand. An Instron 4302 tensile tester with Series IX software was used at a constant gauge length of 250 mm and a cross-head speed of 10 mm / minute. Two tensile tests of each type were performed on each monofilament sample. In all cases, the two resulting stress vs. strain curves were virtually identical. The maximum tensile strength, the maximum strain, and Young's modulus (found by least square fit at the highest slope of the curve) is calculated for each monofilament.

NbTi alloy grain size- The NbTi alloy grain size of restack elements was determined primarily by TEM analysis of transverse cross sections through a subcontract at Sandia National Laboratory. The TEM preparation involved sectioning with an Isomet saw to approximately 0.5 mm thickness, grinding to ~0.12 mm on 600 grit SiC paper, and electropolishing in a solution of 2% hydrofluoric acid, 5% sulfuric acid, and 93% methanol at -60 to -70^0 C. Best electropolishing conditions were 30-40V direct current at 8-14 mA. Bright field images were taken on a Philips CM30 TEM at 300 KV, using a Gatan television camera and an Oxford Instruments Link eXL image analysis system. The resulting 512 x 512 x 256 gray scale black and white image was superimposed on a 15 x 15 line square grid. The reported grain size is taken as a the average intercept distance along the horizontal lines of the grid. Each sample's thin area was analyzed by selected area diffractions to search for α-phase Ti reflections.

Measurements of NbTi grain sizes larger than 1 μm were made on metallurgical mounts made for hardness testing. These mounts were etched used was 1:1:1:5 parts of nitric acid, hydrofluoric acid, lactic acid and de-ionized water, at room temperature for 15 seconds. Images were captured on polaroid film and grain sizes were measured by line intercept method. The reported grain size is taken as the average intercept distance along the grid lines.

X-Ray Line Scans

The JEOL 6100 SEM was used to acquire 256 point line scans across the barrier of select restack element monofilaments from each cable vendor. Windows were made for Nb-$L_{\alpha 1}$, Ti-K_α, and Cu-K_α X-ray peaks to contain approximately 3 sigma for each respective peak. 50 line scans were run and averaged for a total acquisition time of approximately 250 seconds. The line scans for each element were superimposed and the Nb barrier was analyzed for interdiffusion at the Cu/Nb and Nb/NbTi interfaces.

Supported by the Director, Office of Energy Research, Office of High Energy and Nuclear Physics, High Energy Physics Division, U. S. Department of Energy, under contract no. DE-AC02-89ER40486. Manuscript received August 24, 1992.

PP-142

Extrusion K Factor Data

Summaries of the monofilament extrusion data and restack yield data were made at the SSCL. Extrusion k factor is determined from the formula

$$P = k \ln R$$

where P is the run pressure on the back of the billet and R is the area reduction ratio. An average k value was determined for each cable vendor's primary and secondary alloy source material.

Overview of Image Analysis Techniques

The degree of the barrier and NbTi "quality" is characterized numerically in this effort by image analysis. An overview of the techniques developed is presented in this section to provide necessary background information and demonstrate the present capabilities of image analysis. A more thorough discussion of image analysis is presented elsewhere[2].

Image analysis was performed using an Oxford Instruments Link eXL system. Light micrographs were captured with a Hitachi KP-M1U CCD camera on a Mitutoyo FS-110 light microscope. Images from from a JEOL 6100 scanning electron microscope, either SEI (secondary electron images) or BEI (backscatter electron images), were grabbed directly. Stored images were 512 x 512 pixels with 256 gray levels for each pixel.

Images with satisfactory brightness and contrast were acquired at suitable magnifications. Often times several frames were averaged prior to grabbing to give the sharpest possible image. A histogram plot of gray level vs. no. of pixels is formed from the image. When sufficient contrast in the image exists, the histogram will have two well separated peaks, one for the feature(s) of interest and one for the matrix. Typically, the gray level at the minimum in the histogram between the peaks is chosen to define the separation of black and white. The image is then transformed into a binary image. The regions of interest are made white in a black matrix for image analysis routines. Some images require a black to white and white to black transformation.

A white region totally surrounded by a black matrix is called a feature in the Link software. By analyzing these white pixels separately, the image analysis routine determines a set of coordinate information as well as shape information. The program calculates the area, perimeter, length, breadth, centroid coordinates and maximum and minimum coordinates, as well as several other values calculated from these parameters.

A series of shape parameters for NbTi filaments can be developed from the shape information, and details are reported elsewhere[1]. Roundness compares area of the feature (NbTi filament) to the area of a perfect circle of a diameter equal to the maximum diameter of the feature. The barrier thickness is defined as the ratio of the barrier area divided by the length of a line formed by removing one layer of pixels at a time from both the inside and outside surfaces of the barrier. This ratio is used to calculate an effective percentage of barrier on the filament. In addition to the shape parameters, the percentage standard deviation of the filament cross sectional area (filament CV) was calculated at final strand size.

α-Ti Precipitate Size and Volume Fraction

The same TEM equipment and similar techniques as described above was used to thin, electropolish and acquire BEI images of the α-Ti / NbTi two phase microstructure of select heat treatment series samples after each heat treatment. TEM images have an inherent problem with variations in brightness due to changes in sample thickness in the field of view of the TEM image. A gaussian blur technique is utilized to even out this brightness variation. A gaussian weighted filter is passed through the stored image which creates a defocused "blur" image with similar brightness variations as the raw image. The defocused image is inverted (the gray level is multiplied by -1 and 255 is added) and added to the raw image to form a new image with corrected uniform brightness while still containing contrast equal to the raw image[1]. An appropriate binary image is obtained and the area of each precipitate is calculated along with the total area fraction of α-Ti in the image.

RESULTS

Table 1 contains averages for Phase IB data for each vendor as well as Phase IA averages for the primary alloy source (TWCA) and the vendors secondary alloy source. Table 1 contains mean value data for hardness, maximum tensile stress, and NbTi alloy grain size for restack elements.

Table 1. Monofilament restack hardness (Hv), maximum stress (Stress), and grain size (GS) for primary (P) and secondary (S) sources of NbTi alloy.

Vendor	Hv/P	Hv/S	Stress/P	Stress/S	GS/P	GS/S
AISA	175	175	910	933	0.11	0.13
FEC	184	179	911	825	0.17	0.16
IGC	149	147	568	550	2.10	4.50
OST	158	162	704	767	0.24	0.21
OTU	188	185	1001	997	0.12	0.12
SEI	182	183	904	877	0.15	0.14
TSC	169		833		0.13	
HIT	174		895		0.15	

Figure 1 contains a plot of the microhardness vs. maximum stress for the NbTi alloy at restack size. Figure 2 contains a plot of Phase IB average micro hardness vs. strain since either extrusion or monofilament anneal for each vendor. Figure 3 contains a plot of NbTi grain size at restack vs. microhardness.

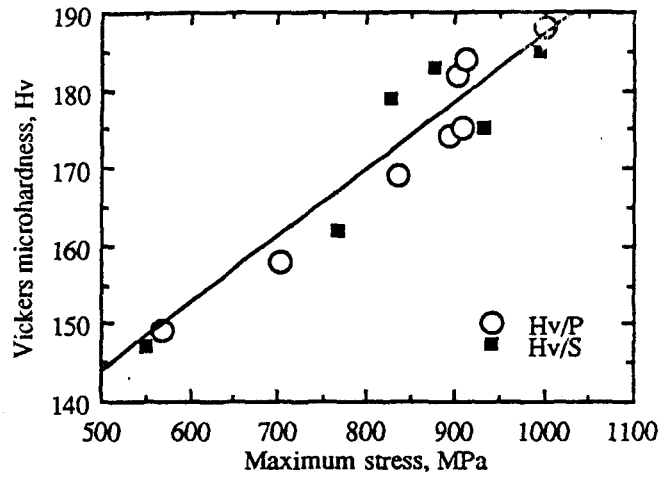

Fig. 1- NbTi alloy Vickers microhardness of monofilament restack elements vs. maximum stress for primary (P) and secondary (S) alloy sources. The line is a linear best fit.

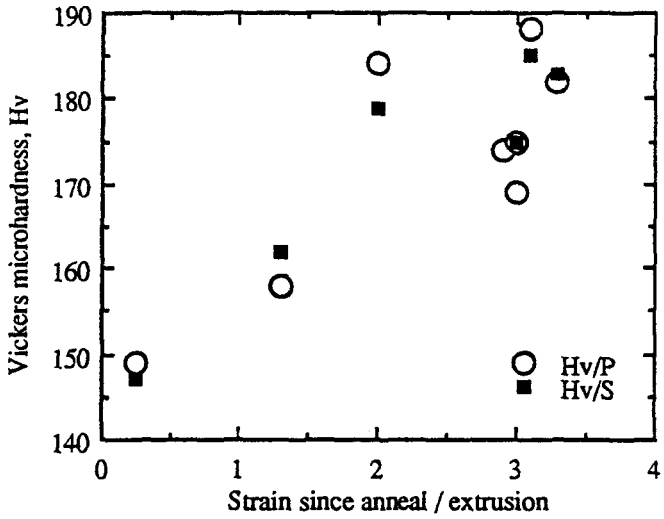

Fig. 2- NbTi alloy Vickers microhardness of monofilament restack elements vs. strain since last anneal or extrusion for primary (P) and secondary (S) alloy sources.

Figure 4 contains the monofilament[3] and multifilament k factor vs. extrusion temperature data for Phase IB material. The average k factor for each vendor's secondary alloy source ranged from a few percent higher to a few percent lower than TWCA material used in Phase IB. The Cv for k factor was about 8% for a typical cable vendor. The Cu/SC ratio is approximately constant at approximately 0.6:1, 1.3:1 and 1.8:1, for the monofilaments, Inner billets, and Outer billets respectively. Therefore, if friction and non uniform deformation can be neglected, one can compare the k factor data on monofilament and multifilament billets to copper flow stress data and extrapolate to obtain a k factor for NbTi alloy. Flow stress data for OFHC copper taken from reference 4 is shown in figure 4 as an estimate of the OFHC copper data k factor. Calculated strain rates for monofilament extrusion are taken to be typically 0.8 s^{-1} at a ram speed of 5 mm /s.

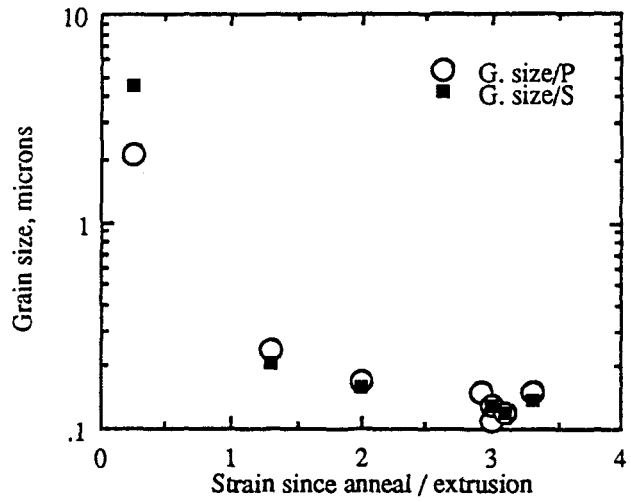

Fig. 3- NbTi grain size of monofilament restack elements vs. strain since anneal or extrusion for primary (P) and secondary (S) NbTi alloy sources.

Using a simple rule of mixtures, the k factor for NbTi alloy can be estimated and is shown by the triangles in figure 4.

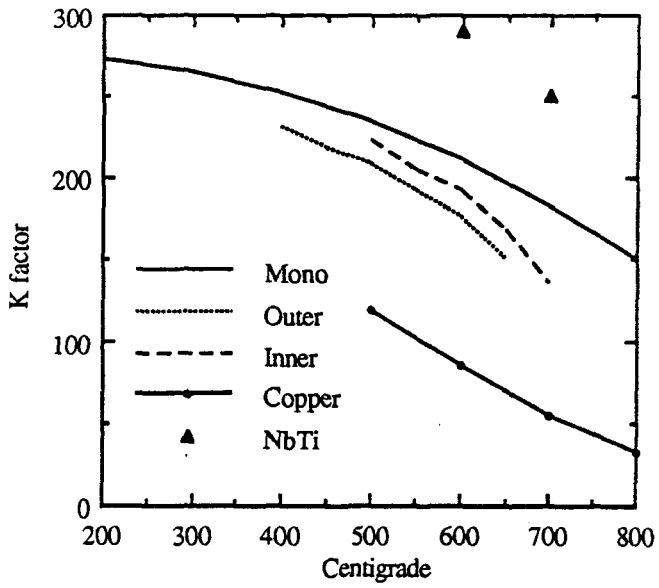

Fig. 4- K factor data for monofilament, Inner composites, Outer composites for Phase IB VQP material. Copper flow stress data are also shown, along with calculated k factor data for NbTi based on rule of mixtures.

Figure 5 shows a typical X-ray line scan for a Nb barrier, along with a secondary electron image showing the physical location of the line. The barrier thickness of the monofilament at restack are on the order of 20 microns for a 4% barrier. A very small level of interdiffusion is observed at the Nb / NbTi interface, which is due in part to the local irregularity of the interface. The interdiffusion seen is on the order of the 0.5 μm X-ray resolution in a SEM. In all cases

studied, the depth of interdiffusion was less than 5 % of the total barrier thickness. The Nb/NbTi interface tended to exhibit a noticeably larger interdiffusion range that that of the Cu/Nb interface. The annealed monofilaments did not show significantly larger interdiffusion than the non-annealed monofilaments, nor were any differences in interdiffusion seen with respect to the Nb sheet vendor.

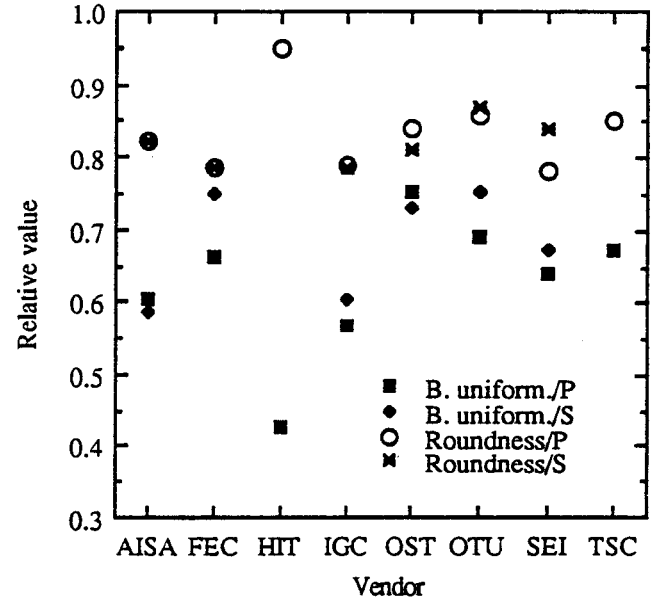

Fig. 6- Restack element image analysis data for primary and secondary alloy sources.

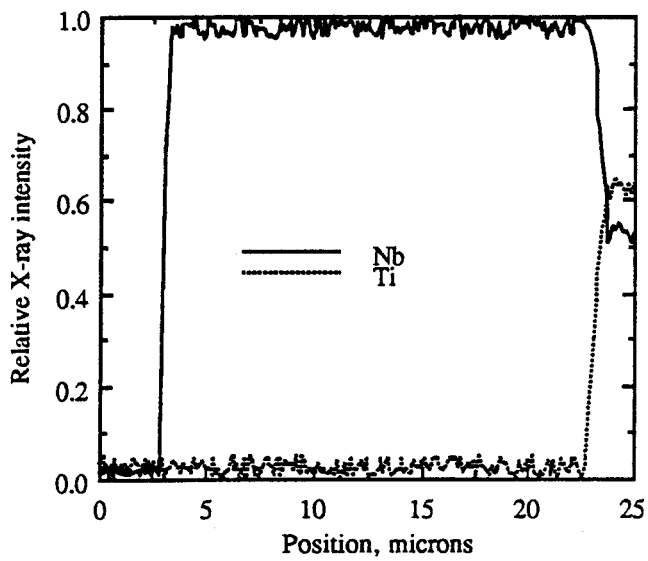

Fig. 5- SEM BEI image (top) showing the location of the line scan and the relative X-ray signals for Nb and Ti. Cu data, not shown for clarity shows no diffusion into the Nb barrier.

Figure 6 shows roundness and barrier uniformity data on restack elements for primary and secondary alloy sources at each vendor. Some NbTi alloy cores show a hexagonal or square like cross sectional shape. The roundness parameter for a perfect hexagon and square are 0.826 and 0.637, respectively. Figure 7 contains images of monofilaments with high (0.96) and low (0.76) values of roundness for comparison. Figure 8 contains roundness and filament Cv data on final size strand.

Fig. 7- Images of non-copper cross sections of restack elements with roundness values of 0.782 (left) and 0.956 (right).

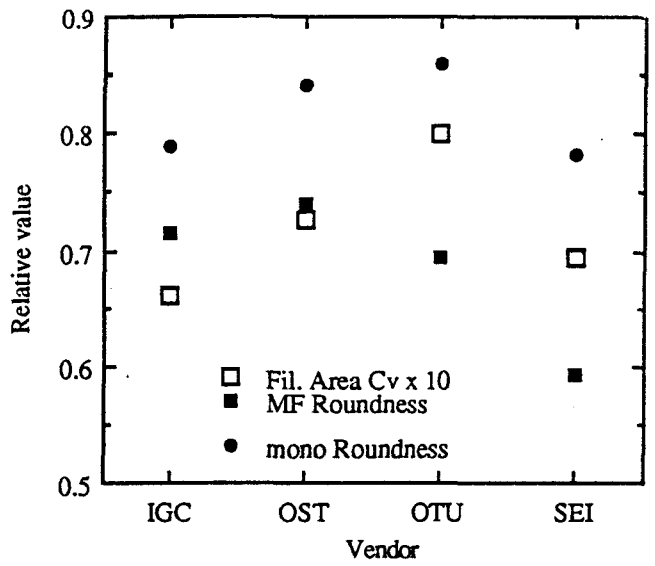

Fig. 8- Phase IB final strand roundness and filament Cv multiplied by 10. The monofilament roundness (filled circles) are shown for comparison.

Figure 9 contains a plot of volume % a-Ti for 5 different heat treatment series from several cable vendors.

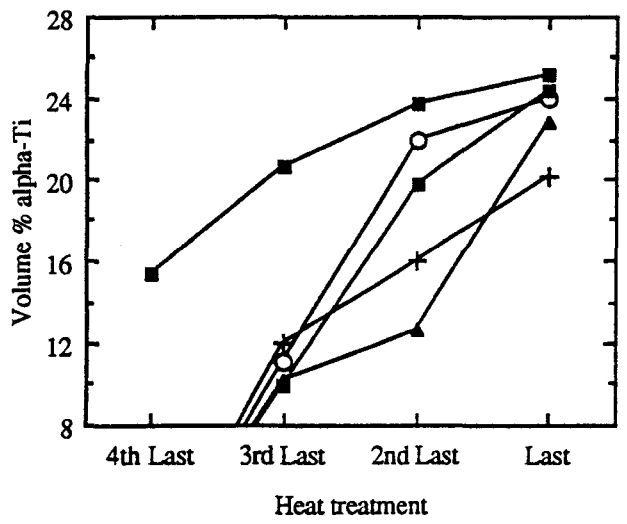

Fig. 9- Volume % α-Ti for 5 different heat treatment series from several cable vendors.

DISCUSSION

The mean hardness data for the monofilaments without anneal ranged from 168 to 186 Hv. Monofilaments having an anneal ranged from 145 to 160 Hv. Hardness was similar for primary and secondary alloy sources.

The maximum tensile stress data for the as-received restack elements ranged from the low 400 MPa's to the low 700 MPa's (data not shown). The non-copper components of these restack elements had considerably higher maximum tensile stress in the range of the mid 500's MPa to 1000 MPa. The ratio of the non-copper maximum stress to the restack maximum stress tended to increase with increasing non copper tensile strength. The monofilament elements that were annealed after extrusion have ratios close to one. This suggests that in the cold work state of the mono annealed material, the mechanical properties of the NbTi and the Cu are more similar.

The elastic modulus values (data not shown) ranges from 44 to 79 GPa, with a Cv of approximately 10% within each vendor. The mean value tended to increase with increasing tensile strength. The elastic modulus for the restack element was similar to the non-copper component. No significant difference in the elastic modulus could be detected between primary and secondary alloy source material within any cable vendor.

The failure strain values (data not shown) were consistently lower for the non-copper components than for the restack elements. The mean values were 3.6 % and 4.2 %, respectively for as-received restack elements and non-copper components. The failure strain tends to increase with increasing maximum tensile stress.

Figures 1, 2, and 3 show the relationships between the NbTi alloy microhardness, tensile strength, grain size, and strain since last anneal. Figure 1 shows a monotonic relationship between hardness and strength. Figure 2 shows that the hardness (and by the correlation in figure 1 the strength) is proportional to the strain since extrusion or last anneal. Figure 2 shows an inverse relationship of grain size to strain since last anneal. In each of these figures, the secondary alloy material behaved similarly to the primary alloy material. Attempts to correlate the extrusion temperatures, reduction ratios, and ram speeds to the variations in hardness or tensile strength were unsuccessful.

The NbTi grain size is very similar for non-annealed material. The mean for all vendors was 0.12 micron with a range of 0.10 to 0.18 micron. This includes both the primary and secondary alloy sources. It should also be noted that these non-annealed materials were processed with a very wide range of monofilament billet diameters, extrusion temperatures, and extrusion reduction ratios. The annealed monofilament grain sizes are variable, but more than twice as large as un-annealed material. In some cases, the grain size exceeded 2 μm. For the samples with grain sizes on the order of 2 μm, light metallographic etches on the NbTi revealed the grain size of the Nb barrier as well. The Nb grains were on the order of 0.3 μm, and apparently are affected by the anneal as well.

Multifilament k factor data shown in figure 4 are consistent with monofilament data, however, one Inner vendor and one Outer vendor's k factor were not used to form the curves. In both of these cases, the temperature or temperature uniformity of the multifilament billets was questionable. The rule of mixtures analysis yielded k factors for NbTi of 290 and 250 at 600 ^{0}C and 700 ^{0}C, respectively with linear correlation coefficients of about 0.95.

X-ray line scan data show negligible interdiffusion of Cu and Ti into the barrier. In some cases, as much as 1 micron of Ti interdiffusion into the Nb barrier could be observed, which is just slightly more that the spatial resolution of X-rays in a tungsten filament SEM. Restack elements that had been annealed after extrusion showed no measurable increase in the amount of interdiffusion over unannealed material.

REST NEEDS WORK----------

The roundness data in Table 4 cover a range of 0.xx to 0.xx. Roundness values tend to be higher for monofilament processes where the extrusion is in a regime of very low temperature or high temperature coupled with a high extrusion reduction ratio. Within some vendors, the roundness values with one alloy source is on the average superior to another alloy source. Over the whole program, no one particular alloy source appears to give superior roundness values. The importance of filament roundness is solely to minimize the perimeter of the filament so as to maximize the barrier thickness at a given barrier volume fraction.

In our other recent work on image analysis, we

We are continuing our efforts on analyzing α-Ti volume fraction at last heat treatment, filament quality and tensile strength at final size. We also plan to quantify the thickness and spacing of the α-Ti precipitates at final strand size, and attempt to correlate all of this data to I_c and piece length data.

ACKNOWLEDGEMENTS

The authors thank T. Tribble for TEM sample preparation , J. R. Michael for TEM BEI imaging, and W. R. Sorenson, and F. A. Gruelich for image analysis. Robert Balliett is acknowledged for supplying the copper flow stress data.

REFERENCES

1). T. J. Headley, J. Michael, F. Greulich, and J. M. Seuntjens, *STEM BSE Imaging and Monte Carlo Simulation of $\alpha-\beta$ Microstructures in NbTi Superconductors*, Proc. of the 50th Annual Meeting of the Electron Microscopy Association of America, 1992.

2). J. M. Seuntjens, F. Y. Clark, T. J. Headley, and N. Wang, Applied Superconductivity Conference, paper LOD-3, 1992, to appear in IEEE-Proceedings, 1993.

3). J. M. Seuntjens, V. A. Bardos, D. W. Capone II, D. Christopherson, F. Y. Clark, E. S. Coleman, M. J. Erdmann, and B. E. Troupe, *Characterization of the Materials from Phase I of the Vendor Qualification Program*, IISSC IV, New Orleans, to appear in Supercollider 4, 1992.

4). Deutsche Gesellschaft Fur Metallkunde E. V., Atlas of Hot Working Properties of Non-Ferrous Metals, Vol. 2, 1978, ISBN 3-88355-001-9.